Chapter 2
Interference Management in Heterogenous Networks

2.1 Introduction

Small cell networks are seen as one of the most promising solutions for boosting the capacity and coverage of wireless networks. The basic idea of small cell networks is to deploy small cells, that are serviced by plug-and-play, low-cost, low-power small cell base stations (SBSs) able to connect to existing backhaul technologies (e.g., digital subscription line (DSL), cable modem, or a wireless backhaul) [1]. Types of small cells include operator-deployed picocells as well as femtocells that can be installed by end users at home or at the office. Recently, small cell networks have received significant attention from a number of standardization bodies including 3GPP [1, 2]. The deployment of SBSs is expected to deliver high capacity wireless access and enable new services for the mobile users while reducing the cost of deployment on the operators. Moreover, small cell networks are seen as a key enabler for offloading data traffic from the main, macrocellular network [3].

The successful introduction of small cell networks is contingent on meeting several key technical challenges, particularly, in terms of efficient interference management and distributed resource allocation [3–5]. For instance, underlying SBSs over the existing macrocellular networks leads to both cross-tier interference between the macrocell base stations and the SBSs and co-tier interference between small cells. If not properly managed, this increased interference can consequently affect the overall capacity of the two-tier network. There are two types of spectrum allocation for the network operator to select. The first type is orthogonal spectrum allocation, in which the spectrum in the network is shared in an orthogonal way between the macrocell and the small cell tiers. Although cross-tier interference can be totally eliminated using orthogonal spectrum allocation, the associated spectrum utilization is often inefficient [3]. The second type is co-channel assignment, in which both the macrocell and the small cell tiers share the same spectrum [4]. As the spectrum in the network is reused through co-channel assignment, the spectrum efficiency can be improved compared to the case of orthogonal spectrum allocation. However, both

© The Author(s) 2017

T. Wang et al., *Overlapping Coalition Formation Games in Wireless Communication Networks*, SpringerBriefs in Electrical and Computer Engineering, DOI 10.1007/978-3-319-25700-6_2

cross-tier interference and co-tier interference should be considered in this case. A lot of recent work has studied the problem of distributed resource allocation and interference management in small cells. These existing approaches include power control [6], fractional frequency reuse [7], interference alignment [8], interference coordination [9], the use of cognitive base stations [10], and interference cancellation [11].

Most existing works have focused on distributed interference management schemes in which the SBSs act noncooperatively. In such a noncooperative case, each SBS accounts only for its own quality of service while ignoring the co-tier interference it generates at other SBSs. Here, the co-tier interference between small cells becomes a serious problem that can significantly reduce the system throughput, particularly in outdoor picocell deployments. To overcome this issue, we enable cooperation between SBSs so as to perform cooperative interference management. The idea of cooperation in small cell networks has only been studied in a limited number of existing work [12–16]. In [12], the authors propose a cooperative resource allocation algorithm on intercell fairness in OFDMA femtocell networks. In [13], an opportunistic cooperation approach that allows femtocell users and macrocell users to cooperate is investigated. In [14], the authors introduce a game-theoretic approach to deal with the resource allocation problem of the femtocell users. In [15], a collaborative inter-site carrier aggregation mechanism is proposed to improve spectrum efficiency in a LTE-Advanced heterogeneous network with orthogonal spectrum allocation between the macrocell and the small cell tiers. The work in [16] propose a cooperative model for femtocell spectrum sharing using a cooperative game with transferable utility in partition form. However, the authors assume that the formed coalitions are disjoint and not allowed to overlap, which implies that each SBS can only join one coalition at most. This restriction on the cooperative abilities of the SBSs limits the rate gains from cooperation that can be achieved by the SBSs. Moreover, the authors in [16] adopt the approach of orthogonal spectrum allocation that is inefficient on spectrum occupation for the two-tier small cell networks.

The goal of this chapter is to develop a cooperative interference management model for small cell networks in which the SBSs are able to participate and cooperate with multiple coalitions depending on the associated benefit-cost tradeoff. We adopt the approach of co-channel assignment that improves the spectrum efficiency compared to the approach of orthogonal spectrum allocation used in [16]. We formulate the SBSs cooperation problem as an overlapping coalitional game and we present a distributed, self-organizing algorithm for performing overlapping coalition formation. Using the presented algorithm, the SBSs can interact and individually decide on which coalitions to participate in and on how much resources to use for cooperation. We show that, as opposed to existing coalitional game models that assume disjoint coalitions, this approach enables a higher flexibility in cooperation. We study the properties of this algorithm, and we show that it enables the SBSs to cooperate and self-organizing into the most beneficial and stable coalitional structure with overlapping coalitions. Simulation results show that this approach yields performance gains relative to both the noncooperative case and the classical case of coalitional games with nonoverlapping coalitions such as in [16].

2.2 System Model

Consider the downlink transmission of an orthogonal frequency division multiple access (OFDMA) small cell network composed of N SBSs and a macrocellular network having a single macro base station (MBS). The access method of all small cells and the macrocell is closed access. Let $\mathcal{N} = \{1, \ldots, N\}$ denote the set of all SBSs in the network. The MBS serves W macrocell user equipments (MUEs), and each SBS $i \in \mathcal{N}$ serves L_i small cell user equipments (SUEs). Let $\mathcal{L}_i = \{1, \ldots, L_i\}$ denote the set of SUEs served by an SBS $i \in \mathcal{N}$. Here, SBSs are connected with each other via a wireless backhaul. Each SBS $i \in \mathcal{N}$ chooses a subchannel set $\mathcal{T}_i$ containing $|\mathcal{T}_i| = M$ orthogonal frequency subchannels from a total set of subchannels $\mathcal{T}$ in a frequency division duplexing (FDD) access mode. The subchannel set $\mathcal{T}_i$ serves as the initial frequency resource of SBS $i \in \mathcal{N}$. The MBS also transmits its signal on the subchannel set $\mathcal{T}$, thus causing cross-tier interference from MBS to the SUEs served by the SBSs. Moreover, the SBSs are deployed in hot spot indoor large areas such as enterprises where there are no walls not only between each SBS and its associated SUEs, but also between all the SBSs. Meanwhile, the MBS is located outdoor, so there exist walls between the MBS and the SBSs.

In a traditional noncooperative scenario, each SBS $i \in \mathcal{N}$ transmits on its own subchannels. The set of the subchannels that SBS i owns is denoted as $\mathcal{T}_i$, where $\mathcal{T}_i \subseteq \mathcal{T}$. SBS i occupies the whole time duration of any subchannel $k \in \mathcal{T}_i$. Meanwhile, the MBS transmits its signal to the MUEs on several subchannels from $\mathcal{T}$, with each MUE occupying one subchannel at each time slot. When the SBSs act noncooperatively, each SBS uses all the subchannels from $\mathcal{T}_i$ to serve its SUEs $\mathcal{L}_i$. For each subchannel $k \in \mathcal{T}_i$, only one SUE $u \in \mathcal{L}_i$ is served on subchannel k. SUE u has access to the full time duration of subchannel k. We denote the channel gain between transmitter j and the receiver u that owns subchannel k in SBS i by g^k_{j,i_u} and the downlink transmit power from transmitter j and the receiver u that occupies subchannel k in SBS i by P^k_{j,i_u}. The rate of SBS $i \in \mathcal{N}$ in the noncooperative case is thus given by

$$\Upsilon_i = \sum_{k \in \mathcal{T}_i} \sum_{u \in \mathcal{L}_i} \log_2 \left(1 + \frac{P^k_{j,i_u} g^k_{j,i_u}}{\sigma^2 + I_{MN} + I_{SN}} \right), \tag{2.1}$$

where σ^2 is the variance of the Gaussian noise, $I_{MN} = P^k_{w,i_u} g^k_{w,i_u}$ is the cross-tier interference from the MBS w to a SUE served by SBS i on subchannel k, and $I_{SN} = \sum_{j \in \mathcal{N}, j \neq i} P^k_{j,i_u} g^k_{j,i_u}$ is the overall co-tier interference suffered by SUE u that is served by SBS i on subchannel k.

We note that, in dense small cell deployments, the co-tier interference between small cells can be extremely severe which can significantly reduce the rates achieved by the SBSs. Nevertheless, due to the wall loss and the long distance between MBS and SUEs, the downlink cross-tier interference is rather weak compared to the co-tier interference between small cells. Thus, in this work, we mainly deal with the downlink co-tier interference suffered by the SUEs from the neighboring SBSs. In order to deal with this interference problem, we allow the SBSs are to cooperate with

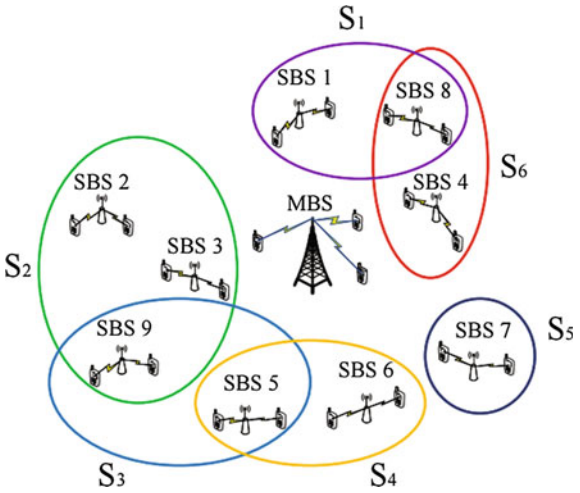

Fig. 2.1 An illustrative example of the cooperative model in small cell networks

one another as illustrated in Fig. 2.1. In such a cooperative network, the SBSs can cooperate to improve their performance and reduce co-tier interference.

2.3 Interference Management as OCF Games

2.3.1 K-Coalition OCF Game Model

Depending on signal-to-noise-plus-interference-ratio (SINR) feedbacks from their SUEs, the SBSs can decide to form cooperative groups called coalitions so as to mitigate the co-tier interference between neighboring SBSs within a coalition. The SBSs can be modeled as the players in a coalitional game. Due to the fact that an SBS may participate in multiple coalitions simultaneously as shown in Fig. 2.1, we consider an OCF game model [17].

The SBSs in the network act as players joining coalitions. A coalition $\mathcal{R} = (\mathbf{R}_1, \ldots, \mathbf{R}_N)$ is a vector in which $\mathbf{R}_i$ is the subset of player i s resource set distributed to this coalition. The support of a coalition $\mathcal{R}$ is defined as $\mathcal{C}(\mathcal{R}) = \{i \in \mathcal{N} | \mathbf{R}_i \neq \emptyset\}$. After joining a coalition $\mathcal{R}$, SBS $i \in \mathcal{C}(\mathcal{R})$ allocates part of its frequency resource into this coalition $\mathcal{R}$. Within each coalition $\mathcal{R}$, the SBSs can jointly coordinate their transmission so as to avoid the collisions. The resource pool of coalition $\mathcal{R}$ is defined as $\mathcal{T}_{\mathcal{R}} = \cup_{i \in \mathcal{C}(\mathcal{R})} \mathbf{R}_i$.

Without loss of generality, we consider that, whenever a coalition $\mathcal{R}$ successfully forms, the transmissions inside $\mathcal{R}$ will be managed by a local scheduler using the time division multiple access (TDMA) approach. The subchannels in $\mathcal{T}_{\mathcal{R}}$ are divided into several time-slots. Each SBS can access only a fraction of all the time-slots when transmitting on a specific subchannel. By doing so, the whole superframe duration

of each subchannel can be shared by more than one SBS. Hence, the downlink transmissions from each SBS in the coalition to its SUEs are separated. Consequently, no more than one SBS will be using the same subchannel on the same time-slot within a coalition, thus efficiently mitigating the interference inside the coalition $\mathcal{R}$. However, as the resource pools of different coalitions may not be disjoint, the system can still suffer from inter-coalition interference. Here, we note that this approach is still applicable under any other coalition-level interference mitigation scheme.

Specifically, we assume the resource pool $\mathcal{T}_{\mathcal{R}}$ of a coalition $\mathcal{R}$ is divided among the SBSs in $\mathcal{R}$ using a popular criterion named proportional fairness, i.e., each SBS $i \in \mathcal{C}(\mathcal{R})$ gets an share $f_i \in [0, 1]$ of the frequency resources from the coalition $\mathcal{R}$ through the TDMA scheduling process of the local scheduler, and the share satisfies that $\sum_{i\in\mathcal{C}(\mathcal{R})} f_i = 1$ and $f_i/f_j = |\mathbf{R}_i|/|\mathbf{R}_j|$. The proportional fairness criterion guarantees that the SBSs that dedicate more of its own frequency resources, i.e., subchannels to the coalition deserve more frequency resources back from the resource pool of the coalition. The gain of any coalition $\mathcal{R} \in CS$, which corresponds to the sum rate achieved by $\mathcal{R}$, is dependent on not only the members of $\mathcal{R}$ but also the coalitional structure CS due to inter-coalition interference. Formally, we define

$$U(\mathcal{R}, CS) = \sum_{i\in\mathcal{C}(\mathcal{R})} \sum_{k\in\mathcal{T}_i} \sum_{u\in\mathcal{L}_i} \gamma^k_{i,i_u} \log_2\left(1 + \frac{P^k_{i,i_u} g^k_{i,i_u}}{\sigma^2 + I_{MO} + I_{SO}}\right), \tag{2.2}$$

where γ^k_{i,i_u} denotes the fraction of the time duration during which SBS i transmits on channel k to serve SUE u, $I_{MO} = P^k_{w,i_u} g^k_{w,i_u}$ denotes the cross-tier interference from the MBS w to SUE u served by SBS i on subchannel k and $I_{SO} = \sum_{\mathcal{R}'\in CS, \mathcal{R}'\neq\mathcal{R}} \sum_{j\in\mathcal{C}(\mathcal{R}'), j\neq i} P^k_{j,i_u} g^j_{w,i_u}$ denotes the overall co-tier interference suffered by SUE u that is served by SBS i on subchannel k.

While cooperation can lead to significant performance benefits, it is also often accompanied by inherent coordination costs. In particular, for the considered SBS cooperation model, we capture the cost of forming coalitions via the amount of transmit power needed to exchange information. In each coalition $\mathcal{R}$, each SBS $i \in \mathcal{C}(\mathcal{R})$ broadcasts its data to the other SBSs in the coalition. Here, each SBS needs to transmit the information to the farthest SBS in the same coalition. We assume that, during information exchange, no transmission errors occur. So the power cost incurred for forming a coalition $\mathcal{R}$ is $P_{\mathcal{R}} = \sum_{i\in\mathcal{C}(\mathcal{R})} P_{i,j^*}$, where where P_{i,j^*} is the power spent by SBS i to broadcast the information to the farthest SBS j in a coalition $\mathcal{R}$. Meanwhile, for every coalition $\mathcal{R}$, we define a maximum tolerable power cost P_{lim}. Therefore, we define the value function of a coalition $\mathcal{R}$ as follows:

$$v(\mathcal{R}, CS) = \begin{cases} U(\mathcal{R}, CS), \text{ if } P_{\mathcal{R}} \leq P_{lim}, \\ 0, \qquad\quad \text{otherwise}, \end{cases} \tag{2.3}$$

Therefore, the payoff that each SBS i achieves from coalition $\mathcal{R}$ is $p_i(\mathcal{R}, CS) = f_i v(\mathcal{R}, CS)$, and the total payoff of SBS i is then $x_i(CS) = \sum_{\mathcal{R}\in CS} p_i(\mathcal{R}, CS)$.

Table 2.1 Algorithm for Interference Management in HetNets

Initial State: The network consists of noncooperative SBSs, and the initial coalitional structure is denoted as $CS = \{\{\mathcal{T}_1\}, \ldots, \{\mathcal{T}_N\}\}$.
$*$ **repeat**
1. Each SBS i discovers its nearby coalitions in the current coalition structure CS, the set of which is denoted by $\mathcal{N}_i$
2. SBS i finds a feasible transformation from the current coalition structure CS to a new coalition structure CS' by reallocating its resources among coalitions in $\mathcal{N}_i$, such that $x_i(CS) < x_i(CS')$
3. SBS i reallocate its resources and the network transforms to a new coalition structure CS'
$*$ **until** the network converges to a stable coalition structure CS^*

2.3.2 *Coalition Formation Algorithm*

We note that the interference management in heterogenous networks is modeled as a K-coalition OCF game, where K is limited by the number of SBSs and the network topology. Based on the framework in Table 1.2, we give a distributed OCF algorithm to achieve a stable outcome of the K-coalition OCF game.

Definition 4 Given a set of player $S \subseteq \mathcal{N}$, we define a complete, reflexive, and transitive binary relation $\preceq_S$ on S over the set of all coalition structures, such that $CS_P \preceq_S CS_Q$, if and only if, we have $x_i(CS_P) \leq x_i(CS_Q)$ for any player $i \in S$.

Therefore, CS_Q is preferred to CS_P for the set of players S if no player's payoff is decreased by transforming CS_P to CS_Q. Based on these relationship, we can define a transform operation for the network. Formally, if the set of players S can transform the coalition structure from CS_P to CS_Q by reallocating their resources, and CS_Q is preferred to CS_P by the same set of players S, then, there exists a feasible transform from CS_P to CS_Q. Due to the communication cost, we restrict the set S as a single SBS and give a coalition formation algorithm as in Table 2.1.

This iterative algorithm starts from an initial state where each SBS forms a single coalition by devoting its own resources. Then, at each iteration, SBS i discovers the nearby coalitions through environment sensing [18], finds a feasible and profitable transform by using the defined relationship $\preceq_{\{i\}}$ and reallocates its resources to perform the transformation. The network converges when there is no feasible and profitable transform for any SBS, and outputs a stable coalition structure CS^*. Given the stable coalition structure CS^*, each SBS i devotes the corresponding resources $\mathbf{R}_i$ to each coalition $\mathcal{R} \in CS^*$. For each coalition $\mathcal{R} \in CS^*$, the coalition members $\mathcal{C}(\mathcal{R})$ coordinate with each other by rescheduling their transmissions with TDMA using the resource pool $\mathcal{T}_{\mathcal{R}}$.

2.3.3 Simulation Results

For simulations, we consider an MBS that is located at the chosen coordinate of (1 km, 1 km). The radius of the coverage area of the MBS is 0.75 km. The number of MUEs is 10. N SBSs are deployed randomly and uniformly within a circular area around the MBS with a radius of 0.1 km. There is a wall loss attenuation of 20 dB between the MBS and the SUEs, and no wall loss between the SBSs and the SUEs. Each SBS has a circular coverage area with a radius of 20 m. Each SBS has 4 subchannels to use and serves 4 users as is typical for small cells. The total number of subchannels in the considered OFDMA small cell network is 20. The bandwidth of each subchannel is 180 kHz. The total number of time-slots in each transmission in TDMA mode is 4. The transmit power of each SBS is set at 20 dBm, while the transmit power of the MBS is 35 dBm. The maximum tolerable power to form a coalition $P_{lim} = 100$ dBm. The noise variance is -104 dBm.

In Fig. 2.2, we present a snapshot of an OFDMA small cell network resulting from the given algorithm with $N = 7$ SBSs. The radius of the distribution area of SBSs is 0.7 km. The cooperative network shown in this figure is a stable coalitional structure CS^*. Initially, all the SBSs schedule their transmissions noncooperatively. After using the OCF algorithm, they self-organize into the structure in Fig. 2.2. This coalitional structure consists of 5 overlapping coalitions named Coalition 1, Coalition 2, Coalition 3, Coalition 4, and Coalition 5. The support of Coalition 1 consists of SBS 3 and SBS 6. The support of Coalition 2 includes SBS 2 and SBS 5. The support of Coalition 3 includes SBS 1 and SBS 6. The support of Coalition 4 includes SBS

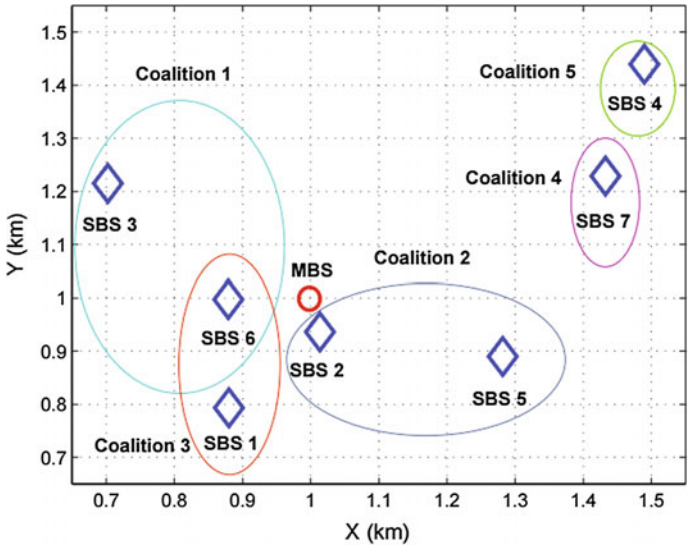

Fig. 2.2 A snapshot of an overlapping coalitional structure resulting from the considered approach in a small cell network

7. The support of Coalition 5 includes SBS 4. SBS 4 and SBS 7 have no incentive to cooperate with other SBSs as their spectral occupation is orthogonal to all nearby coalitions. Meanwhile, SBS 6 is an overlapping player because its resource units are divided into two parts assigned to different coalitions. The interference is significantly reduced in CS^* as compared to that in the noncooperative case, as the interference between the members of the same coalition is eliminated using proper scheduling. Clearly, Fig. 2.2 shows that by adopting the OCF algorithm, the SBSs can self-organize to reach the final network structure.

Figure 2.3 shows the overall system utility in terms of the total rate achieved by the OCF algorithm as a function of the number of SBSs N compared with two other cases: the nonoverlapping coalition formation (CF) algorithm and the noncooperative case. Figure 2.3 shows that for small networks ($N < 4$), due to the limited choice for cooperation, the OCF algorithm and the CF algorithm have a performance that is only slightly better than that of the noncooperative case. This indicates that the SBSs have no incentive to cooperate in a small-sized network as the co-tier interference remains tolerable and the cooperation possibilities are small. As the number of SBS N increases, the possibility of cooperation for mitigating interference increases. Figure 2.3 shows that, as N increases, the OCF algorithm exhibits improved system performances compared to both the traditional coalition formation game and that of the noncooperative case. The performance advantage reaches up to 32 and 9 % at $N = 10$ SBSs relative to the noncooperative case and the classical CF case, respectively.

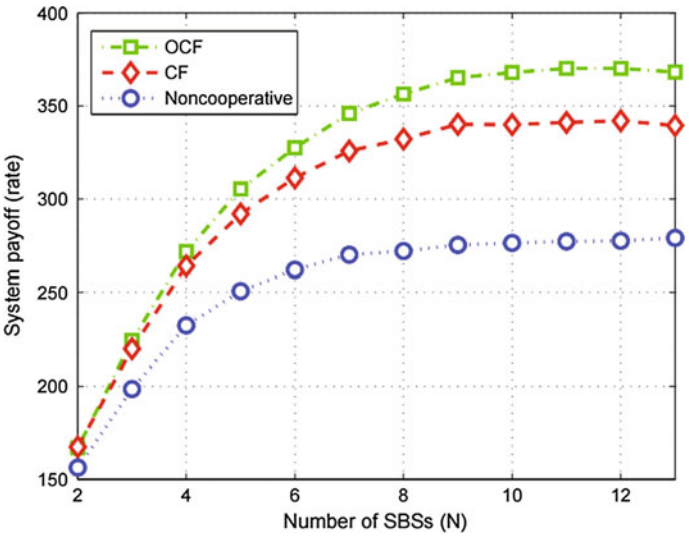

Fig. 2.3 Performance evaluation in terms of the overall system payoff as the number of SBSs N varies

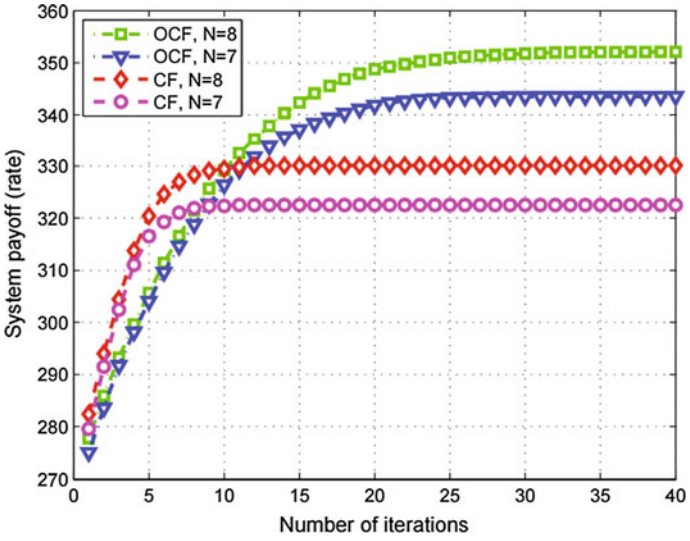

Fig. 2.4 System payoff versus number of iterations

Figure 2.4 shows the convergence process under different scenarios using the OCF algorithm and the CF algorithm. We observe that, although the OCF algorithm requires a few additional iterations to reach the convergence as opposed to the CF case when both $N = 7$ and $N = 8$, this number of iterations for OCF remains reasonable. Moreover, Fig. 2.4 shows that the OCF algorithm clearly yields a higher system payoff than the CF case, with only little extra overhead, in terms of the number of iterations. Hence, the simulation results in Fig. 2.4 clearly corroborate our earlier analysis.

Figure 2.5 shows the cumulative density function (CDF) of the individual SBS payoff resulting from the OCF algorithm and the CF algorithm when the number of SBSs is set to $N = 10$. From Fig. 2.5, we can clearly see that the OCF algorithm performs better than the CF algorithm in terms of the individual payoff per SBS. For example, the expected value of the individual payoff for a network formed from the OCF algorithm is 36, while for a network formed from the CF algorithm the expected value is 33. This is due to that the OCF algorithm allows more flexibility for the SBSs to cooperate and form coalitions. Each SBS is able to join multiple coalitions in a distributed. way by adopting our OCF algorithm, while it can only join one coalition at most in the CF case. Moreover, during each reallocation, the SBSs improve their own payoff without being detrimental to the other SBSs in the new coalition. This also contribute to a growth of the individual payoff of each SBS. In a nutshell, Fig. 2.5 shows that the OCF algorithm yields an advantage on individual payoff per SBS over the CF algorithm.

Figure 2.6 shows the growth of the system payoff of the network as the number of SBSs increases, under different maximum tolerable power costs of a coalition P_{lim}.

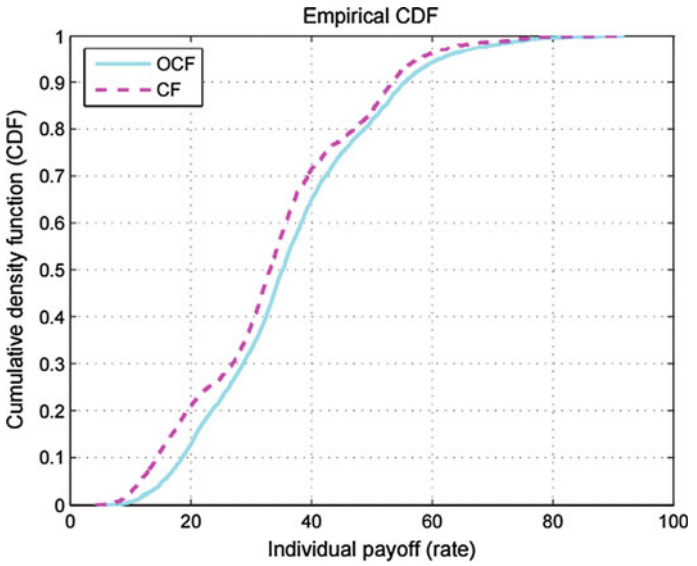

Fig. 2.5 Cumulative density function of the individual payoff for a network with $N = 10$ SBSs

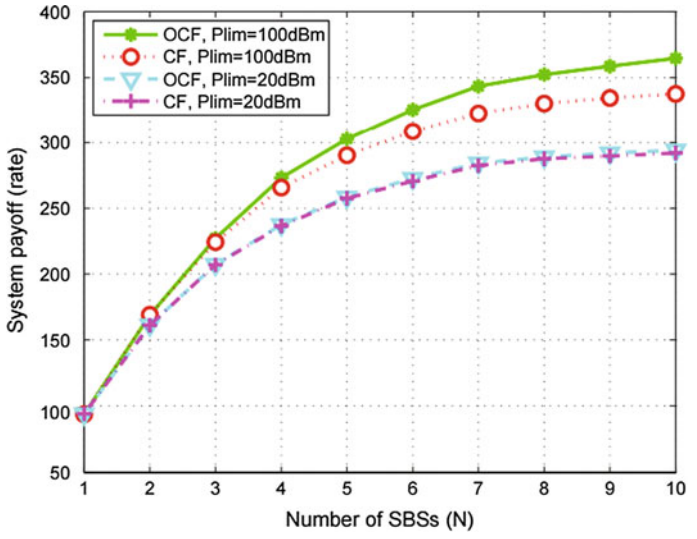

Fig. 2.6 System payoff as a function of number of SBSs N, for different maximum tolerable power costs

Both the OCF algorithm and the CF case are considered in Fig. 2.6. We observe that, as the number of SBSs increases, the system payoff under two conditions both grows. Moreover, the OCF algorithm has a small advantage on the system payoff compared to the CF case when $P_{lim} = 20$ dBm, while the advantage of the OCF algorithm over the CF case is more significant when $P_{lim} = 100$ dBm. This is due to the fact that when P_{lim} is low, the SBSs can hardly cooperate with other neighboring SBSs. Most SBSs choose to stay alone as the power cost of possible coalitions exceeds the maximum tolerable power cost. Thus, the system payoff of the OCF algorithm and of the CF algorithm are close. Furthermore, when P_{lim} is high, each SBS is able to reallocate its SBS units to join neighboring coalitions and improve both the system payoff and its own payoff using the OCF algorithm. Meanwhile, the cooperation possibility of the SBSs under the CF case is also increased when P_{lim} increases. Consequently, Fig. 2.6 shows that the OCF algorithm incurs a higher probability for the SBSs to cooperate than the CF case, especially when the maximum tolerable power cost of forming a coalition is high. Thus, our OCF algorithm achieves better system performances in terms of sum rate than the CF algorithm.

Figure 2.7 shows the relationship between the number of coalitions that each SBS joins and the number of SBSs under the OCF case and the CF case. As the number of SBSs increases, both the maximum and the average number of coalitions that each SBS joins also grows under the OCF case. While in the CF case, each SBS is only allowed to join one coalition at most no matter how the number of SBSs changes, thus causing the maximum number and the average number of coalitions that each SBS joins to remain the same when the number of SBSs increases. Figure 2.7 shows that the incentive toward cooperation for the SBSs is more significant for the

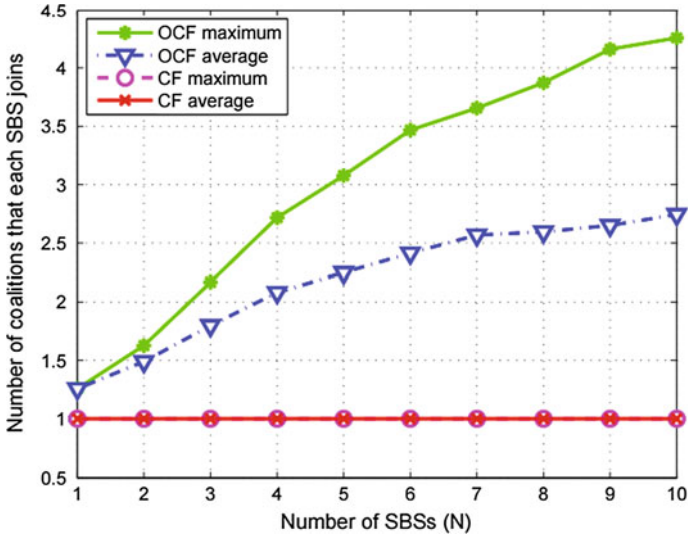

Fig. 2.7 Number of coalitions per SBS as a function of number of SBSs N

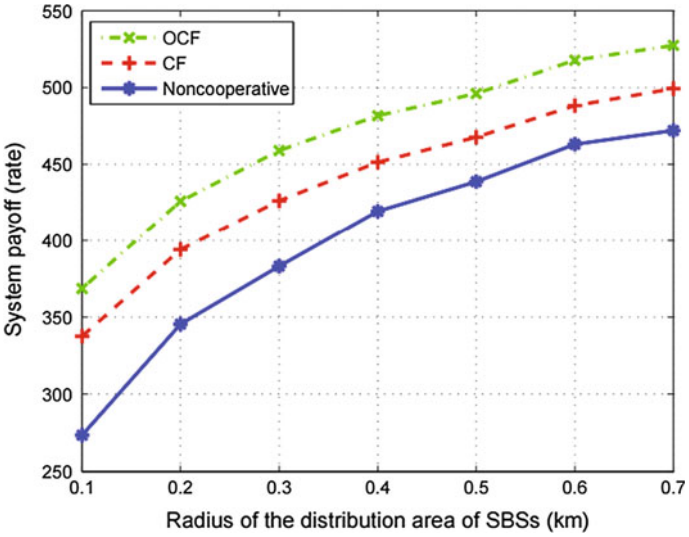

Fig. 2.8 System payoff versus radius of the distribution area of SBSs for a network with $N = 10$ SBSs

OCF algorithm than for the CF case. Thus, The cooperative gain can be achieved more efficiently by using our OCF algorithm than the CF case when the SBSs are densely deployed in the network. The cooperative probability of the OCF algorithm represented by the maximum number of coalitions that each SBS joins is 325.75 % larger than that of the CF case when $N = 10$ SBSs are deployed in the network.

In Fig. 2.8, we show the system payoff in terms of sumrate as the radius of the distribution area of SBSs varies. The number of SBSs in the network is set to $N = 10$. We compare the system payoff of the OCF algorithm, CF case and noncooperative case. Figure 2.8 shows that as the radius of the distribution area of SBSs increases, the system payoff also increases. This is because both the co-tier interference and the cross-tier interference are mitigated when the SBSs are deployed in a larger area. Thus, the system payoff is improved for the OCF algorithm, the CF case as well as the noncooperative case. From Fig. 2.8, we can also observe that as the radius of the distribution area of SBSs varies, our OCF algorithm yields a higher system payoff than the CF case and the noncooperative case.

In Fig. 2.9, we continue to compare our OCF approach to the CF case and the noncooperative case in terms of system payoff as the total number of the available subchannels in the network changes. Here, $N = 10$ SBSs are deployed in the network. Note that, we adopt the approach of co-channel assignment, i.e., the SBSs reuse the spectrum allocated to the macrocell. Figure 2.9 shows that the system payoff of the OCF algorithm, the CF case, and the noncooperative case are improved when the total number of available subchannels increases. This is due to the fact that when the number of available subchannels increases, the probability of conflicts on subchannels is greatly decreased. Thus, the interference in the two-tier small cell

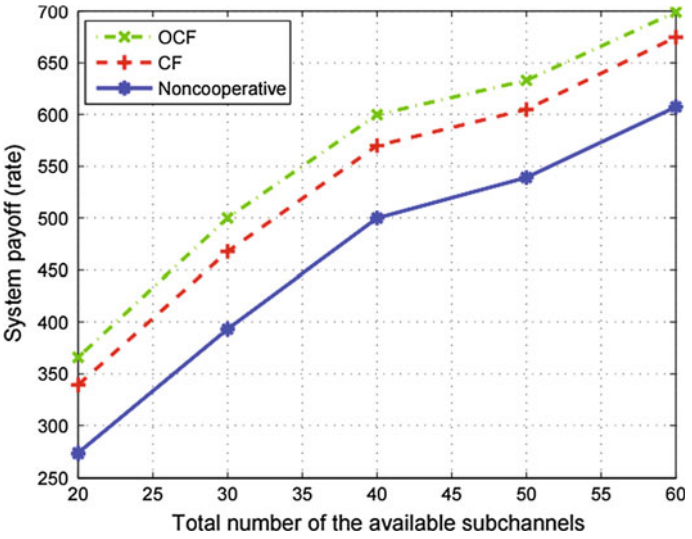

Fig. 2.9 System payoff versus total number of subchannels for a network with $N = 10$ SBSs

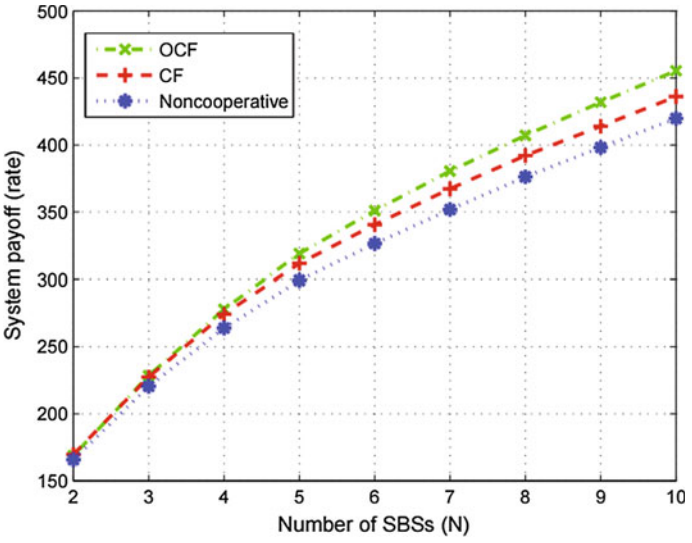

Fig. 2.10 Performance evaluation in terms of the overall system payoff with wall loss in the small cell tier as the number of SBSs N varies

network is mitigated, causing the improvement of the system payoff in terms of sum rate. Moreover, Fig. 2.9 shows that the OCF algorithm outperforms the CF case and the noncooperative case in terms of system payoff when the total number of available subchannels increases.

In Fig. 2.10, we modify the scenario by considering the wall loss between the MBS and the SUEs and the wall loss between the SBSs and the SUEs, both of which are set at 20 dB. In this scenario, the downlink cross-tier interference has a much greater impact on system performance than in the scenario where no wall exists between the SBSs and the SUEs such as in Fig. 2.3. As shown in Figs. 2.3 and 2.10, the advantage on system payoff of our OCF algorithm over the CF algorithm and the noncooperative case when no wall loss is considered between the SBSs and the SUEs is more significant than that when wall loss is involved.

2.4 Summary

In this chapter, we have investigated the problem of cooperative interference management in small cell networks. We have formulated this problem as an overlapping coalition formation game between the small cell base stations. Then, we have shown that the game has a transferable utility and exhibits negative externality due to the co-tier interference between small cell base stations. To solve this game, we have presented a distributed overlapping coalition formation algorithm that allows the small cell base stations to interact and individually decide on their cooperative decisions. By adopting this algorithm, each small cell base station can decide on the number of coalitions that it wishes to join as well as on the resources that it allocates to each such coalition, while optimizing the tradeoff between its overall rate and the associated cooperative costs. We have shown that the OCF algorithm is guaranteed to converge to a stable coalition structure in which no small cell base station has an incentive to reallocate its cooperative resources. Simulation results have shown that the overlapping coalitional game approach allows the small cell base stations to self-organize into cooperative coalitional structures while yielding notable rate gains relative to both the noncooperative case and the classical coalition formation algorithm with nonoverlapping coalitions.

References

1. T.Q.S. Quek, G. de la Roche, I. Guvenc, M. Kountouris, *Femtocell Networks: Deployment, PHY Techniques, and Resource Management*. (Cambridge University Press, Cambridge, 2013)
2. J.G. Andrews, H. Claussen, M. Dohler, S. Rangan, M. Reed, Femtocells: Past, Present, and Future. IEEE J. Sel. Areas Commun. **30**(3), 497–508 (2012)
3. D. Lopez-Perez, A. Valcarce, G. de la Roche, J. Zhang, OFDMA Femtocells: a roadmap on interference avoidance. IEEE Commun. Mag. **47**(9), 41–48 (2009)
4. D. Calin, H. Claussen, H. Uzunalioglu, On femto deployment architectures and macrocell offloading benefits in joint macro-femto deployments. IEEE Commun. Mag. **48**(1), 26–32 (2010)
5. Y.S. Liang, W.H. Chung, G.K. Ni, I.Y. Chen, H. Zhang, S.Y. Kuo, Resource allocation with interference avoidance in OFDMA femtocell networks. IEEE Trans. Veh. Technol. **61**(5), 2243–2255 (2012)

6. V. Chandrasekhar, J. Andrews, Z. Shen, T. Muharemovic, A. Gatherer, Power control in two-tier femtocell networks. IEEE Trans. Wirel. Commun. **8**(8), 4316–4328 (2009)
7. J.Y. Lee, S.J. Bae, Y.M. Kwon, Interference analysis for femtocell deployment in OFDMA systems based on fractional frequency reuse. IEEE Commun. Lett. **15**(4), 425–427 (2011)
8. N. Lertwiram, P. Popovski, K. Sakaguchi, A study of trade-off between opportunistic resource allocation and interference alignment in femtocell scenarios. IEEE Commun. Lett. **1**(4), 356–359 (2012)
9. S. Randan, R. Madan, Belief propagation methods for intercell interference coordination in femtocell networks. IEEE J. Sel. Areas Commun. **30**(3), 631–640 (2012)
10. J. W. Huang, V. Krishnamurthy, Cognitive base stations in LTE/3GPP femtocells: a correlated equilibrium game-theoretic approach. IEEE Trans. Commun. **59**(12), 3485–3493 (2011)
11. M. Wildemeersch, T.Q.S. Quek, M. Kountouris, C.H. Slump, Successive interference cancellation in uplink cellular networks, in *Proceedings 2013 IEEE SPAWC*, Darmstadt, Germany (2013)
12. K. Lee, O. Jo, D.H. Cho, Cooperative resource allocation for guaranteeing intercell fairness in femtocell networks. IEEE Commun. Lett. **15**(2), 214–216 (2011)
13. R. Urgaonkar, M.J. Neely, Opportunistic cooperation in cognitive femtocell networks. IEEE Trans. Veh. Technol. **30**(3), 607–616 (2012)
14. O.N. Gharehshiran, A. Attar, V. Krishnamurthy, Collaborative sub-channel allocation in cognitive LTE femto-cells: a cooperative game theoretic approach.IEEE Trans. Commun. **61**(1), 325–334 (2013)
15. B. Soret, H. Wang, K.I. Pedersen, C. Rosa, Multicell cooperation for LTE-advanced heterogeneous network scenarios. IEEE Wireless Commun. **20**(1), 27–34 (2013)
16. F. Pantisano, M. Bennis, W. Saad, R. Verdone, M. Latva-aho, Coalition formation games for femtocell interference management: a recursive core approach, in *Proceedings of the IEEE Wireless Communication Network Conference*, Quintana-Roo, Mexico (2011)
17. Z. Zhang, L. Song, Z. Han, W. Saad, Coalitional games with overlapping coalitions for interference management in small cell networks. IEEE Trans. Wireless Commun. **12**(5), 2659–2669 (2014)
18. A. Zalonis, N. Dimitriou, A. Polydoros, J. Nasreddine, P. Mahonen, Femtocell downlink power control based on radio environment maps, in *Proceedings of the IEEE Wireless Communication Network Conference*, Paris, France (2012)

http://www.springer.com/978-3-319-25698-6

Overlapping Coalition Formation Games in Wireless Communication Networks

Wang, T.; Song, L.; Saad, W.; Han, Z.

2017, IX, 67 p. 24 illus., Softcover
ISBN: 978-3-319-25698-6